Concentration of mercury and other metals in an Arctic planktonic food web under a climate warming scenario

Asiedu, Delove Abraham; Søndergaard, Jens; Jónasdóttir, Sigrun; Juul-Pedersen, Thomas; Koski, Marja

Published in:
Marine Pollution Bulletin

Link to article, DOI:
10.1016/j.marpolbul.2023.115436

Publication date:
2023

Document Version
Publisher's PDF, also known as Version of record

Marine Pollution Bulletin 194 (2023) 115436

Contents lists available at ScienceDirect

Marine Pollution Bulletin

journal homepage: www.elsevier.com/locate/marpolbul

Concentration of mercury and other metals in an Arctic planktonic food web under a climate warming scenario

Delove Abraham Asiedu [a,*], Jens Søndergaard [b], Sigrun Jónasdóttir [a], Thomas Juul-Pedersen [c], Marja Koski [a]

[a] National Institute of Aquatic Resources, Technical University of Denmark, DK-2800 Kgs. Lyngby, Denmark
[b] Department of Ecoscience, Arctic Research Centre, Aarhus University, Frederiksborgvej 399, DK-4000 Roskilde, Denmark
[c] Greenland Climate Research Center, Greenland Institute of Natural Resources, Nuuk 3900, Greenland

ARTICLE INFO

Keywords:
Arctic
Plankton
Hg
Heavy metals
Biomagnification

ABSTRACT

Arctic marine ecosystems act as a global sink of mercury (Hg) and other metals, and high concentrations of these have been measured in higher trophic-level organisms. Nevertheless, the concentrations of metals at the basis of the marine food web in the Arctic is less known despite the likelihood of biomagnification from dietary sources. We investigated the concentrations of mercury (Hg) and other metals in different size fractions of plankton in West Greenland. All size fractions contained detectable levels of Hg (ranging from 4.8 to 241.3 ng g dw^{-1}) at all stations, although with high geographic variability, likely reflecting the sources of mercury (e.g., meltwater). In many cases, the concentrations in the larger-size fractions were lower than in the smaller-size fractions, suggesting depuration through the metabolic activity of mesozooplankton. Concentrations of Cd, Pb, V, Ni, and Cr were higher than previously reported elsewhere in the Arctic.

1. Introduction

Heavy metals, including cadmium (Cd), lead (Pb), chromium (Cr), nickel (Ni) and mercury (Hg), are naturally occurring elements in our environment. However, these elements could become biohazards at high concentrations. For example, Pb and methylmercury (MeHg), the organic form of Hg, are regarded as neurotoxic even at low exposure concentrations, whereas Cd, Ni and Cr are carcinogenic and/or allergenic (Manić et al., 2022; Schwaba et al., 2021; Zulaikhah et al., 2020). Of these metals, Hg, Pb, and Cd are considered critical from environmental and human health perspectives (Marnane, 2018; Steffen et al., 2005; World Health Organisation, 2017). This is due to their (1) high toxicity, (2) ability for long-range atmospheric transport (particularly Hg) and (3) potential to bioaccumulate and biomagnify in both humans and animals (Chen et al., 2012; Chouvelon et al., 2019; Krabbenhoft and Sunderland, 2013; Hermanson and Brozowski, 2005).

Globally, emissions of Hg, Cd and Pb into the atmosphere and depositions in aquatic ecosystems have increased several folds since the onset of industrialisation (AMAP, 2011; McConnell and Edwards, 2008). Due to their persistent nature, these metals can bioaccumulate in living organisms, which increases the concentrations and toxic effects in higher trophic levels (Chouvelon et al., 2019; Harding et al., 2018). For instance, monitoring of ringed seals, toothed whales and seabirds in West Greenland and Canada has shown a ten-fold increase in Hg concentrations over the past 150 years (Dietz et al., 1996; Dietz et al., 2009). Also, high Cd and Pb concentrations have been found in the kidneys of Greenlandic ringed seals and sea birds (Bjerregaard et al., 2004; Johansen et al., 2006). This is of particular concern since fish and marine mammals are important local sources of protein (Troell et al., 2017), and fish and shrimp are key export products of Greenland (https://stat.gl). Indeed, an increased level of Hg up to 40 μg L^{-1} has been measured in the blood of Greenlandic adults (AMAP, 2009). This concentration is several times higher than the United States Environmental Protection Agency's recommended safe threshold of 5.8 μg Hg L^{-1} and could thus critically affect human health (AMAP, 2011; Lehnherr, 2014). Also, blood Pb concentrations of up to 352 μg L^{-1}, three times higher than the world health organization's recommendation of 50–100 μg L^{-1}, have been measured in some Greenlandic adults (Bjerregaard et al., 2004).

Arctic marine ecosystems, although having limited local sources of contaminants, are particularly vulnerable to pollution by Hg and other contaminants with air-born transport (Bergmann et al., 2022; Kirk et al., 2012). Hg is released into the atmosphere either as Gaseous Elemental

* Corresponding author.
E-mail address: delas@aqua.dtu.dk (D.A. Asiedu).

https://doi.org/10.1016/j.marpolbul.2023.115436
Received 15 June 2023; Received in revised form 15 August 2023; Accepted 17 August 2023
Available online 1 September 2023

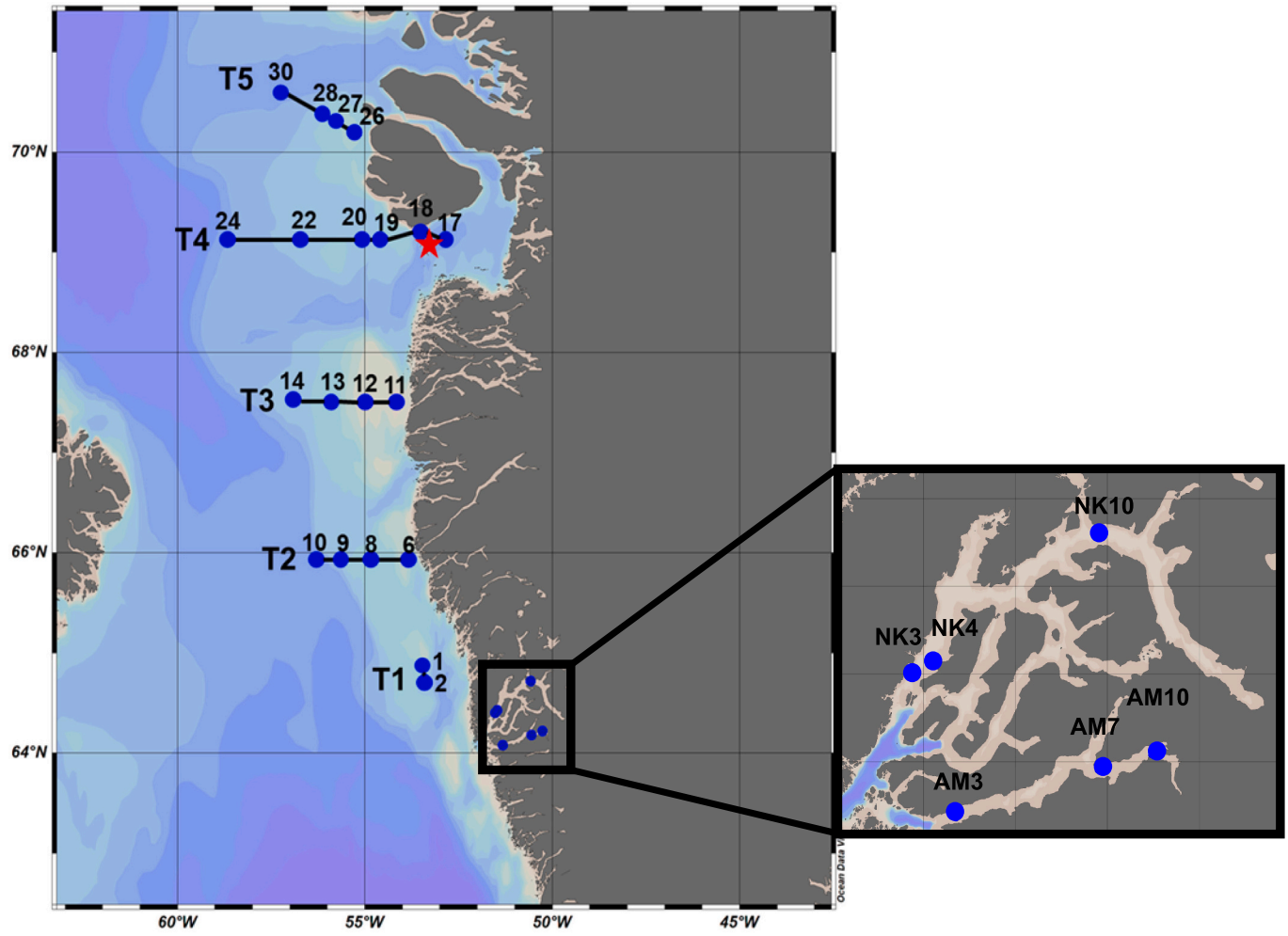

Fig. 1. Sampling stations (blue circles) along the five onshore-offshore transects (T1- T5), the fjord stations in Ameralik (AM) and Nuup Kangerlua (NK) and the additional station in Disko Bay (red star) off West Greenland. The station numbers along the transects correspond to the stations reported by Munk et al. (2022) and the station numbers in Ameralik and Nuup Kangerlua to the monitoring stations of Greenland Institute for Natural Resources (Stuart-Lee et al., 2021). The station in Disko Bay corresponds to the station of the Greenland Ecosystem 202 Monitoring (GEM) program (http://data.g-e-m.dk). (For interpretation of the references to colour in this figure legend, the reader is referred to the web version of this article.)

Mercury (GEM), which has a long atmospheric residence time of about 1.2 years and can be transported over longer distances, or Reactive Gaseous Mercury (RGM), which has a short residence time, travels over a short distance and is readily scavenged from the atmosphere. The vulnerability of Arctic marine ecosystem to Hg contamination is partly due to a quasi-stationary atmospheric event (blocking), which triggers the transport of GEM and other contaminants from the mid-latitudes to the Arctic, especially during the winter and early spring (Bradley et al., 1992; Iversen and Joranger, 1985; Stohl, 2006; Steffen et al., 2008). Open water leads and polynyas in the Arctic release reactive halogens, mainly bromine (Br), which readily oxides GEM to RGM, which are readily scavenged by the Arctic ice and snow (Gabrielli and Vallelonga, 2015). Although some Hg is emitted back into the atmosphere as GEM through photoreduction, continuous scavenging and accumulation of RGM leads to the accumulation of Hg reserves in snow and ice, with concentrations higher than in the atmosphere (Chételat et al., 2022). Moreover, Schuster et al. (2018) estimated that, on average, Arctic permafrost soils contain 1656 Gg of Hg, nearly two folds higher than present in all other soils, oceans, and atmosphere combined. Hawkings et al. (2021) measured concentrations of dissolved Hg in sub-glacial melts from Greenland Ice Sheets that were among the highest recorded for natural water bodies, although these measurements are currently debated (Jørgensen et al., 2022).

Concentrations of Pb and Cd in Greenland ice cores are ca. 60-fold higher than during the pre-industrial period (Candelone et al., 1995; McConnell and Edwards, 2008; McConnell et al., 2019), although atmospheric concentrations of Pb and Cd have reduced in recent decades (Pawlowska and Charvat, 2004). Pb and Cd occur either as aerosol elements or attached to aerosol materials (Hermanson and Brozowski, 2005) and have an atmospheric residence time of 4–9 days, sufficient for transport to Arctic areas.

In light of the rapid melting of Arctic ice and the thawing of permafrost due to climate warming, freshwater run-offs from the Arctic cryosphere to coastal Arctic ecosystems are projected to increase by nearly 10–30 % by the end of 2100 (Walsh et al., 2005). Since run-offs are associated with liberated legacy Hg, Cd, and Pb, among other metals, increasing discharges might alter the metal concentrations in Arctic marine ecosystems, with unknown consequences for biological processes (Chételat et al., 2022; Miner et al., 2021). Hence, it has become imperative to monitor Hg and other metals in Arctic marine ecosystems to understand and predict their trends, evaluate their effects on Arctic marine biota, and safeguard food security and public health (AMAP, 2018; UN Environment, 2019).

Marine plankton constitutes the basis of the pelagic food web and is the primary energy source for higher trophic-level organisms (Macdonald and Bewers, 1996). In addition, marine plankton plays a critical

role in the recycling and transport of metals, including Hg, Cd and Pb, in the pelagic food web (Kehrig and do A., 2011). Zhang et al. (2018) and González-Dávila (1995) have shown a strong correlation between the concentrations of heavy metals in the water column and their biological uptake by marine phytoplankton. When the phytoplankton is ingested by zooplankton, the metals can be (1) retained in their tissues and transferred to higher trophic level organisms, depending on exposure time and concentration as well as on trait-based characteristics such as prosome length, lipid volume and developmental stage of zooplankton, (2) egested as faecal pellets and transported to deeper waters, or (3) excreted in dissolved form increasing the residence time of metals in the water column (Achary et al., 2020; Xu and Wang, 2003; Yu et al., 2020). The planktonic components of the pelagic food web can thus alter the concentration and distribution pattern of metals in marine ecosystems. Indeed, high Hg concentrations (especially MeHg) measured in fishes and mammals originate mainly from lower trophic levels (Chen et al., 2012), with biomagnification factors of 2.1–15.1 from phytoplankton to zooplankton (Li et al., 2022) and up to 69 from zooplankton to marine fishes (Harding et al., 2018). Similarly, bioaccumulation of other heavy metals, including Pb, Cd, Cr and Cu from plankton to fish, has been reported (Zhang et al., 2016), with bioaccumulation factors being a magnitude higher in zooplankton than in phytoplankton (Chevrollier et al., 2022) and 1.5–84.4 from zooplankton to fish (Zhang et al., 2016).

Despite the evidence pointing towards a dietary pathway as the primary source of Hg and other metals in higher trophic levels (Matias et al., 2022), only a few studies have examined their concentrations in Arctic plankton (Fox et al., 2017; Pućko et al., 2015). We quantified the concentration of total Hg in different size fractions of marine plankton from the west coast of Greenland to investigate 1) the geographic variability of concentrations and biomagnification of Hg in Arctic plankton and 2) how it is shaped by the environmental factors and plankton community structure. In addition, we 3) compared the Hg concentration in mesozooplankton to the concentration of other metals/metalloids (As, Cr, Cd, Pb, Ni, and V). Our results display the current metal levels and contribute to understanding the bioaccumulation and biomagnification of Hg and other metals at the base of the Arctic marine food web, which is essential to assess the magnitude and effects of contamination in the changing Arctic.

2. Materials and methods

2.1. Study area

The study was conducted along five onshore-offshore transects between latitudes of 64^0 N (Nuuk) and 70^0 N (Disko Bay) and in two fjords, Ameralik and Nuup Kangerlua (64^0 N, 52^0 W) off the west coast of Greenland (Fig. 1). The transects were sampled between 17th and 30th July 2021, Ameralik fjord and Nuup Kangerlua fjord were sampled on the 6th and 10th of September 2021, and an additional sampling was conducted at Disko Bay (69.14° N, 53.28° W) on the 27 and 30th of March and the 3rd of April 2022.

Marine productivity and biodiversity are high off the coast of West Greenland (Born and Böcher, 2001). The hydrography of the area is largely driven by a mixture of cold, less-saline polar water from the East Greenland Current and saline Atlantic water from the Irminger Current (Christie and Sommerkorn, 2012; Rigét et al., 2018). These water masses form the West Greenland Current (WGC), which controls marine oceanographic conditions and the distribution and composition of marine organisms in the region (Buch, 2002; Buch et al., 2004; Rykova et al., 2015). In addition, the WGC triggers a major upwelling during the spring period, bringing nutrient-rich bottom water to the photic zone, resulting in high primary production (Castelao et al., 2019). The northernmost study area, Disko Bay, is located at the southern border of the Arctic Sea ice. The bay is influenced by sub-Arctic and Arctic waters and has pronounced seasonality in sea ice cover, with ice formation mostly from late October to early November and ice cover until May–June (Møller and Nielsen, 2020). The plankton community composition changes from south to north with increasing concentrations of Arctic species. Primary producers are dominated by diatom species such as *Corethron criophilum, Actinocyclus* cf. *octonarius* and *Thalassiosira spp,* whereas consumers are dominated by copepod species such as *Calanus finmarchicus, Calanus hyperboreus, Calanus glacialis, Metridia longa, Pseudocalanus elongatus, Acartia longiremis, Oithona similis and Microcalanus pusillus* (Munk et al., 2003).

Both of the investigated fjords receive meltwater from the Greenland Ice Sheet and riverine discharges towards the open ocean (Meire, 2016). Nuup Kangerlua has an area of 2013 km^2, making it one of the largest Greenlandic fjords in terms of surface area. The fjord receives freshwater from land-terminating glaciers and marine subglacial melt waters, contributing to elevated nutrient replenishment and pelagic primary production in summer (Juul-Pedersen et al., 2015). Ameralik Fjord is a comparatively small fjord (surface area of 400 km^2) adjacent to Nuup Kangerlua (Meire et al., 2015; Mortensen et al., 2020). However, in contrast to its adjacent fjord, freshwater input is only from the land terminating glaciers (Greenland Ice sheets) via a glacier river, making the two fjords distinctly different (Møller et al., 2006). Plankton in fjord ecosystems are dominated by phytoplankton assemblages of diatoms (*Thalassiosira spp),* haptophytes (*Phaeocystis* spp) and dinoflagellates (*Gymnodinium* spp. and *Gyrodinium* spp.; Krawczyk et al., 2015, 2018) and by zooplankton assemblages of copepod species including *Calanus* spp., *Microsetella norvegica, Pseudocalanus* spp. and *Metridia longa* (Arendt et al., 2010). Physicochemical parameters and, to a large extent, the biology of these fjords are expected to change due to the increasing influx of water from subglacial melts in response to climate-induced warming (Meire et al., 2017; Mortensen et al., 2020; Stuart-Lee et al., 2021). This makes them important models for studying the impact of climate change on marine ecosystems.

2.2. Sampling

Plankton samples for Hg analyses from the transect stations were collected for four different size fractions (>200, 50–200, 20–50 and 0.7–20 μm) onboard R/V Dana (Institute for Aquatic Resources, Technical University of Denmark) as part of a cruise of the Horizon 2020 project ECOTIP (Munk et al., 2022). In addition, similar size fractions were collected from three stations in Ameralik fjord and three stations in Nuup Kangerlua fjord onboard a small research vessel Avataq (Greenland Institute of Natural Resources) and from an ice-covered station in Disko Bay. Samples for As, Cd, Ni, Cr, Pb and V analyses were collected for the >200 μm size fraction from the transect stations.

For plankton size fractions >200 μm, samples were collected by oblique hauls (0–100 m depths) of a 200-μm meshed plankton net attached to a ring net with a diameter of 3.5 m and 1 m long cod end attached to midwater ring nets (Ayala et al., 2018). These hauls were conducted at all stations, except stations 3 and 4, fjords stations and the Disko Bay station in March, where a 200-μm WP2 plankton net was used. The WP2 net was pulled vertically at a speed of ca. 0.5 m s^{-1} from 10 m below the chlorophyll-*a* maximum layer to the surface at stations 3 and 4 and at fjord stations and from 100 m to the surface at the Disko Bay station. All samples collected from these nets were concentrated onto acid-washed 200 μm mesh filters (diameter of 9 cm). For plankton size fractions of 50–200 μm, vertical hauls of a 50-μm WP2 plankton net from ca. 10 m below the chlorophyll-*a* maximum layer to the surface were conducted similarly to the vertical hauls with the 200 μm net. These samples were first filtered through a 200 μm mesh filter and then concentrated onto acid-washed pieces of a 50-μm mesh filter. The 200 μm mesh filter was stored and used to analyse the other metals. For the 20–50 μm size fractions, a 20 μm phytoplankton net was towed horizontally at a speed of ca. 1.5 knots for ca. 2 min at a depth of ca. 1–2 m. Similar to 50–200 μm samples, the 20–50 μm samples were first filtered through a 50 μm mesh filter and then concentrated onto acid-washed 20 μm mesh filters. However, due to strong wind and high waves at most

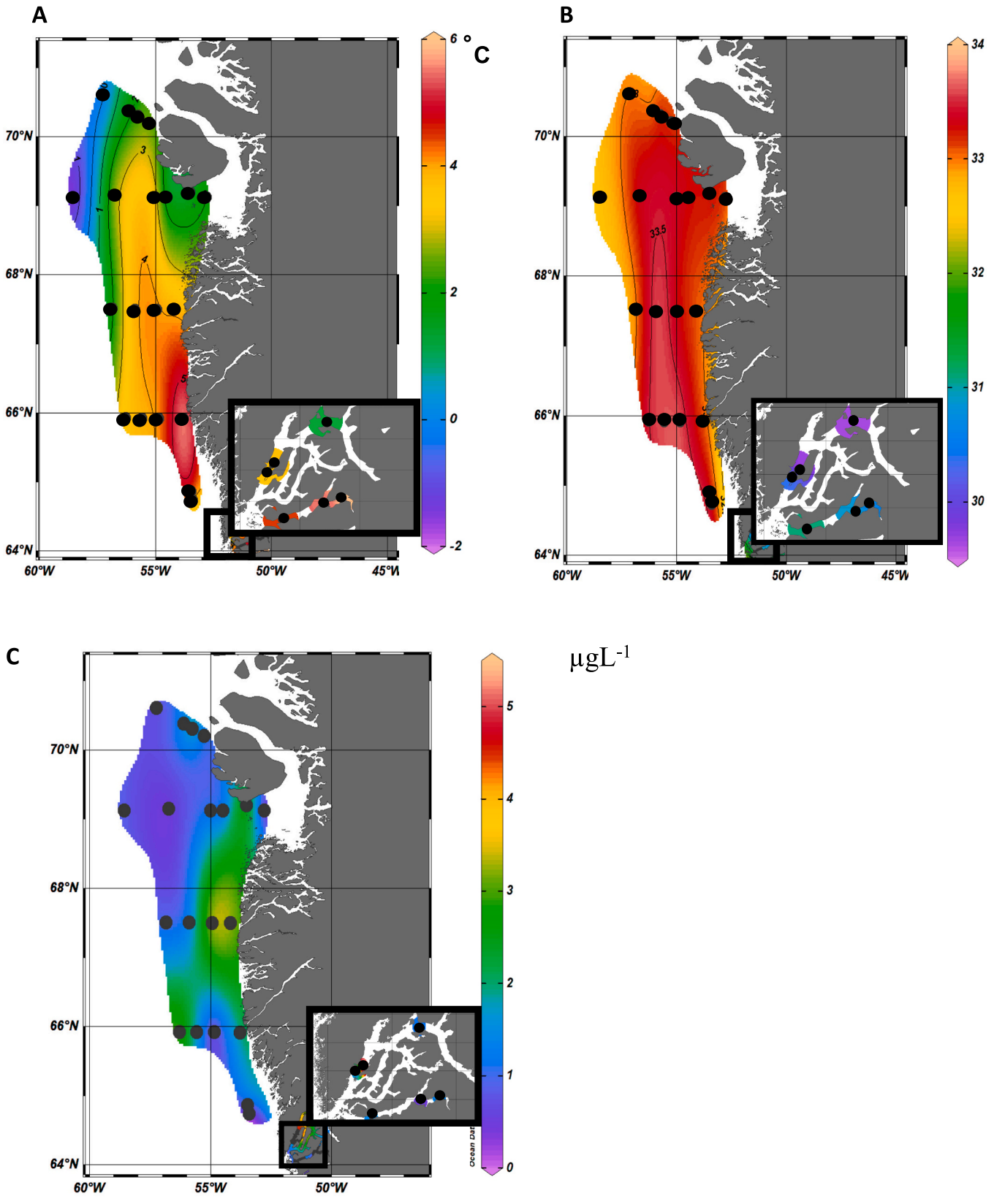

Fig. 2. Average temperature (A; °C), salinity (B) and chlorophyll-*a* concentration (C; µg L^{-1}) at the sampling depths at the transect and fjord stations. Stations corresponding to Fig. 1 are shown as black dots. The different colour gradients represent the intensity of temperature, salinity and chlorophyll-*a*.

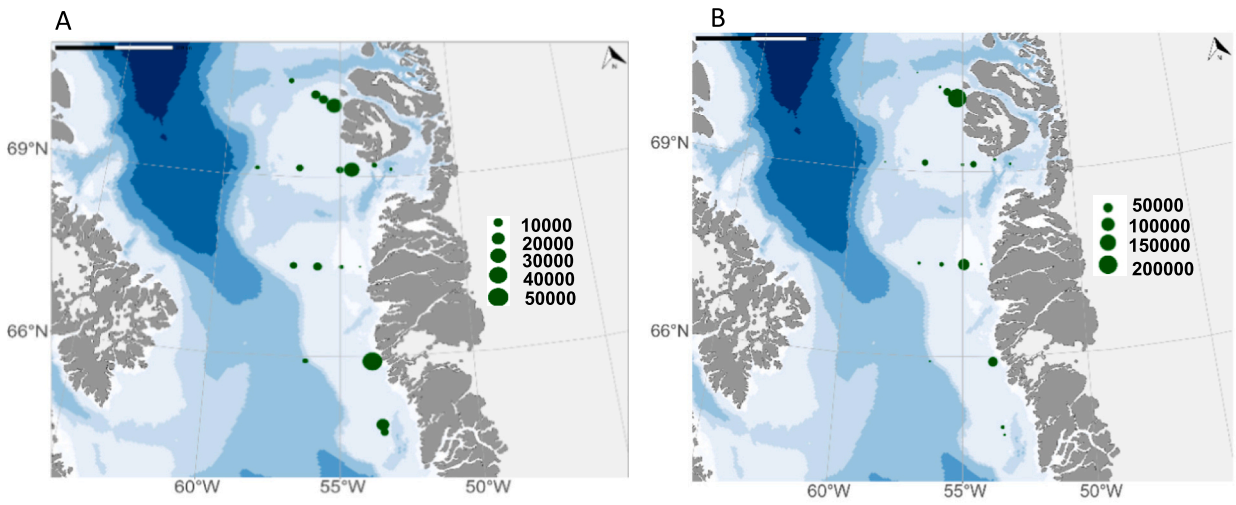

Fig. 3. Average abundance (ind. m^{-3}) of (A) zooplankton ≥200 μm and B) zooplankton ≤200 μm at the transect stations. The size of the circle indicates the average abundance. The blue colour indicates the depth. (For interpretation of the references to colour in this figure legend, the reader is referred to the web version of this article.)

transect stations, collection by 20 μm net was only possible at stations 3 and 4 and in the fjord stations. At the remaining stations, filtrates from the 50 μm WP2 plankton nets were concentrated onto a 20 μm net to collect any plankton in the size fraction of 20–50 μm that may have been retained by the 50 μm net due to net clogging. Plankton samples of 0.70–20 μm were collected from the Chlorophyll-*a* maximum depth (ca. 20–30 m) using Niskin bottles mounted on a CTD rosette. The water was sieved through a 20 μm net and concentrated onto combusted GF/F filters (Whatman). All filters were placed into Petri-dishes, sealed to avoid contamination and frozen at −20 °C until analyses. All nets, cod ends, and glass wear were soaked in 10 % HCl for 24 h and rinsed twice with Milli-Q water before use.

Concurrently, depth profiles of temperature, salinity and fluorescence were obtained using a CTD (SBE 911plus) and water samples were collected for chlorophyll-*a* analysis from distinct depths (Suppl. Table 2) at the surface 100 m. Vertical samples for the community composition and abundance of zooplankton were collected at transect stations using a multinet midi (Hydrobios) with five nets of 50 μm mesh size. These samples were preserved in a 2 % formaldehyde for later species identification.

2.3. Sample analyses

Total Hg was measured in plankton in the 20–50, 50–200 and > 200 μm size fractions using a Direct Mercury Analyzer (DMA; Milestone) at the Department of Ecoscience, Aarhus University, following the US-EPA Method 7473. Prior to analyses, filters were freeze-dried and the sample was gently scraped off the filters using a spatula and placed into porcelain mortar, homogenized and transferred into nickel boats of the DMA for THg analyses. The analytical quality was controlled by concurrently analysing aqueous standard solutions (10 ng and 100 ng of Hg), procedural blanks, duplicates, and Certified Reference Materials (CRM) BCR-414 (plankton), DORM-4 (fish protein) and NIST-1515 (apple leaves). Measurements were corrected for instrumental drift using the control standard solutions (drift was always <10 %). All samples were corrected for concurrent blanks. Duplicates showed an RSD mean ± SD of 9 ± 9 % (n = 14). Measured recoveries of the CRMs (mean ± SD) were 94 ± 1 % (n = 8) for BCR-414, 102 ± 3 % for DORM-4 (n = 11) and 105 ± 2 % (n = 3) for NIST-1515. The laboratory is accredited by the Danish Accreditation Fond DANAK to a detection limit of 1 ng $(g\ dw)^{-1}$.

Total Hg in the 0.7–20 μm size fractions and other metals/metalloids were measured using an Inductively Couple Plasma Mass Spectrometer (ICP-MS; Agilent 7900) at the Department of Ecoscience, Aarhus University. Prior to analyses, filters with the samples were digested in half-concentrated nitric acid following the DS 259 standard using an Anton Paar Multiwave 7000 microwave oven and digestion solutions diluted with Milli-Q water. Blank filters (n = 3) and the CRMs, BCR-414 and NIST-1515, were analysed for control. The limit of detection for the metals was determined as 3 SD on the blanks and the CRMs showed a recovery of 89 ± 6 % (n = 3) and 92 ± 16 % (n = 3) for Hg for BCR-414 and NIST-1515, respectively. In addition to the 0.7–20 μm size fractions, remaining samples of the larger plankton size fractions (>200 μm) off the transect stations were also analysed using ICP-MS.

Water samples for chlorophyll-*a* analysis were filtered on a GF/F filter and preserved at −20 °C for later extraction. Chlorophyll-*a* samples from the transect stations were extracted using 96 % ethanol, whereas fjord samples were extracted using 90 % acetone (Sterman, 1988), depending on which extractant was available. Extracts were kept at 4 °C and Chlorophyll-*a* was measured after 24 h using a calibrated fluorometer (Trilogy Laboratory Fluorometer, Model 7200-00).

Zooplankton species and life-stages were identified to the lowest taxonomic levels and counted. The length of 10 individuals of each species and life-stages were measured. All processing of zooplankton samples was conducted by ZooplanktonID.dk. Size measurements (prosome length) were used to estimate the species composition in the different size fractions by separating plankton species into >200 μm and <200 μm size fractions.

2.4. Statistical analysis

The differences in Hg concentrations between the different plankton size fractions and sampling stations within each transect or fjord were analysed using a 2-way analysis of variance (ANOVA) with the station and size fraction as independent variables. In addition, the differences between the size fractions and between the stations were analysed after pooling the data from all stations using a 1-way ANOVA. The differences in the concentrations of other metals (As, Cd, Pb, V, Ni, and Cr) between the transects were estimated after data from the transect stations were pooled using 1-way ANOVA. Metal concentrations were log-transformed if the residuals of the analysis did not present normal distributions using the Shapiro-Wilk test. Tukey pairwise comparison (post hoc test) was used for pairwise comparisons. Canonical correspondence analysis (CCA) was performed to determine the relationship between the

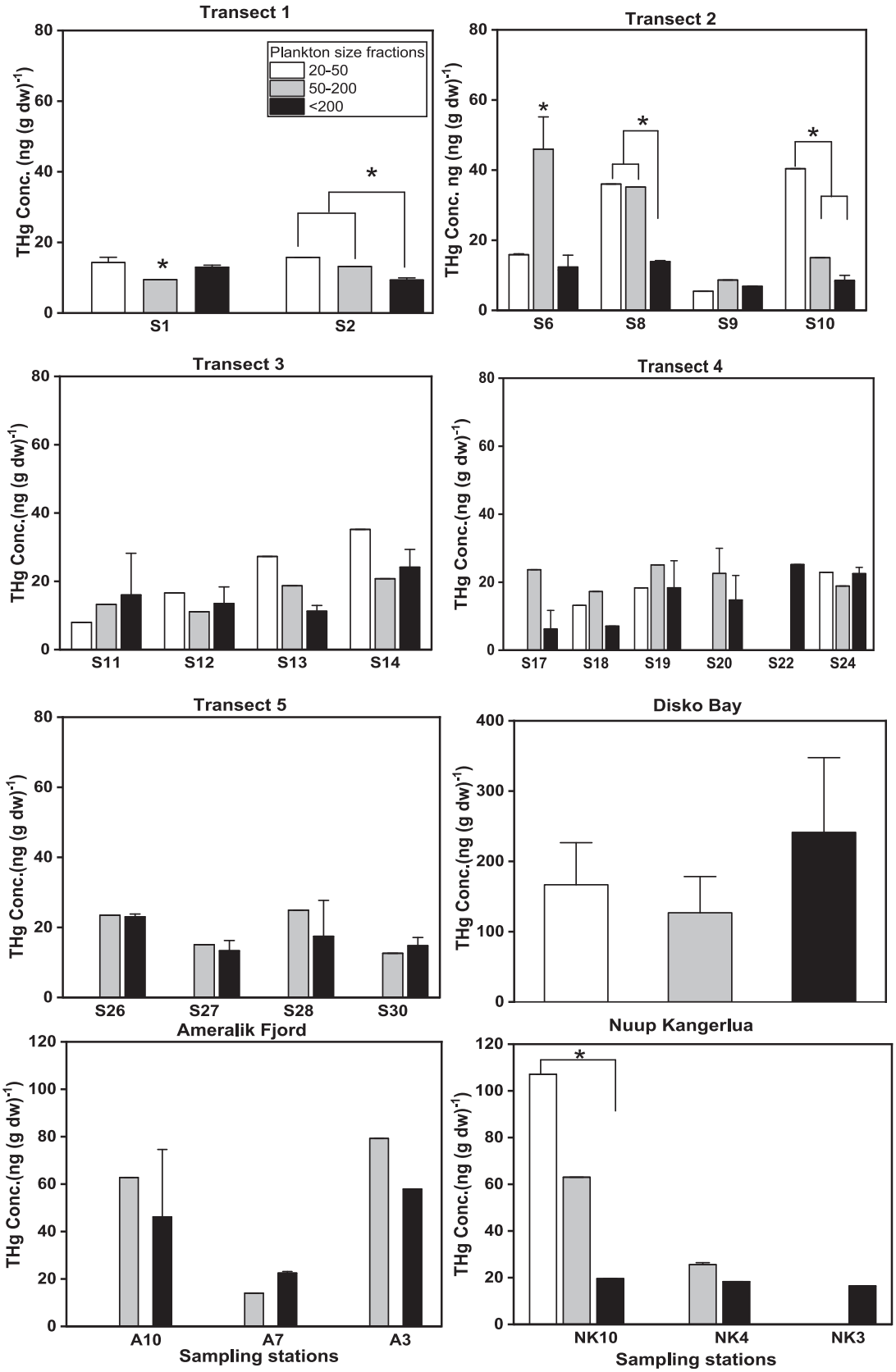

Fig. 4. Total mercury (THg) concentrations (ng (g dw)$^{-1}$) in the different plankton size fractions at the different stations (mean ± SE). (*) Indicates significant differences between the size fractions (Tukey HSD; $p < 0.05$; Suppl. Table 1). (White bars) 20–50 μm, (grey bars) 50–200 μm, (black bars) >200 μm size fraction. Note different scales of the y-axis. The sampling stations correspond to Fig. 1.

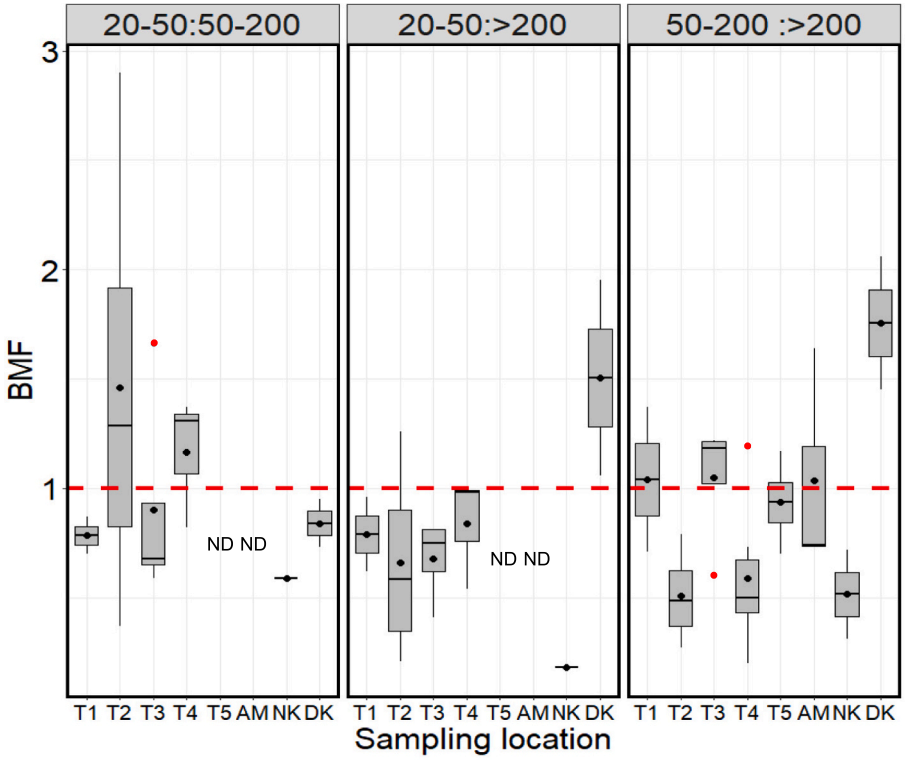

Fig. 5. The average biomagnification factor (BMF) between the different plankton size fractions at the different transects and fjord stations. The box represents 50 % of measurements and whiskers extend 25 % of the box ranges. Values outside this range (red circles) are outliers. Black Horizontal lines represent the median values and the solid black circles indicate the mean. The red dotted horizontal line marks the BMF of 1 (boxes below the line show no biomagnification). (ND) No data. (For interpretation of the references to colour in this figure legend, the reader is referred to the web version of this article.)

concentration of Hg or other metals, zooplankton abundance and environmental variables (temperature, salinity and chlorophyll-*a*). Hierarchical partitioning (HP) analysis was performed to determine the contribution of the abundance of zooplankton species and environmental variance to the metal concentrations using "rdacca.hp" package in R (Lai et al., 2022).

Biomagnification Factor (BMF) was estimated by dividing the metal concentration in the predator (larger size fraction) by the metal concentration in the prey (smaller size fraction; Alava and Gobas, 2012).

3. Results

3.1. Hydrography and zooplankton abundance and community structure

Temperature varied across the sampling stations, with the warmest average temperature (5.3 ± 0.4 °C) observed in Ameralik fjord (September). Generally, the average temperature of the sampling depths at transect stations (July) decreased from 4.3 ± 0.4 °C in the southern to 1.6 ± 0.6 °C in the northern transects (Fig. 2A). The colder surface water was typically less saline than the warmer water below (Fig. 2A &B), and the fjords were less saline than the transects, indicating input of freshwater from riverine and glacial meltwater. Chlorophyll-*a* concentrations were, on average, almost similar in fjords (1.8 ± 0.5 μg L^{-1}) and at transect stations (1.6 ± 0.13 μg L^{-1}, Fig. 2C), and no variation was observed between the southern and northern transects. The upper 100 m in Disko Bay in March–April had an average temperature, salinity, and Chlorophyll-*a* concentration of −1.3 °C, 33.6, and 0.3 μg L^{-1}, respectively.

In general, the abundance of both large (>200 μm) and small (<200 μm) zooplankton increased from the southern to the northern transects, except for a high abundance of 50,000 ind. m^{-3} for both size fractions in one of the southern stations (Fig. 3). Zooplankton abundance was also higher at the stations close to the coast than at the offshore stations, with the abundance of large zooplankton being ca. 2-fold lower than the abundance of small zooplankton. The relative abundance of zooplankton >200 μm was dominated by *Oithona similis, Pseudocalanus* spp., *Calanus* spp., *Triconia borealis* and *Microsetella norvegica* (Suppl. Fig. 1a). Whereas *M. norvegica, Triconia borealis, Calanus* spp., and *Pseudocalanus* spp. increased in proportional abundance from the southern to northernmost stations, *O. similis* was equally abundant in both the southern and northern stations (Suppl. Fig. 1A). The relative abundance of organisms <200 μm was dominated by the bivalve and gastropod larvae and the rotifer *Synchaeta* spp., with their proportional abundances increasing from the southern to the northern stations (Suppl. Fig. 1B). Samples for zooplankton abundance were not taken in the fjord stations, but the Greenland monitoring data indicated that adults and nauplii of *M. norvegica, Calanus* spp., *Pseudocalanus* spp., *Oithona* spp., *Oncaea* spp., and *Microcalanus* spp. typically dominate the zooplankton abundance during July–August (Arendt et al., 2013).

3.2. Total mercury concentrations in plankton

Total Hg concentrations in the different plankton size fractions and stations varied up to 20-fold (Fig. 4). The highest Hg concentration (241.3 ng (g dw)$^{-1}$) was recorded in the >200 μm plankton size fraction in Disko Bay (March–April) and the lowest Hg concentration (4.8 ng (g dw) $^{-1}$) in the same size fraction at the transect station 17 (July). The average Hg concentrations in all size fractions were significantly higher at the fjord stations compared to the transect stations (1 way ANOVA, $F_{1,3} = 52.2$, $P < 0.05$; Tukey HSD; $p < 0.01$) and the concentrations in Disko Bay were significantly higher than the concentrations in both the transect stations and the fjord stations (1 way ANOVA, $F_{1.3} = 52.2$, $p < 0.05$, Tukey HSD, $p < 0.01$).

The average Hg concentrations in the size fractions of >200, 50–200 and >20–50 μm at all stations were 32.9 ± 8.8, 35.7 ± 6.8 and 42.6 ± 13.0 ng (g dw)$^{-1}$ (mean ± SE), respectively. In general, there was no consistent trend in the Hg concentrations between different size fractions, but these varied depending on the stations. For example, Hg concentrations observed at stations 2, 8, 10, 13 and NK10 showed a decreasing trend from the 20–50 to 50–200 and >200 μm plankton size fractions. In contrast, the concentrations in most stations in transects 3, 4 and 5 and in Disko Bay were not significantly different between the

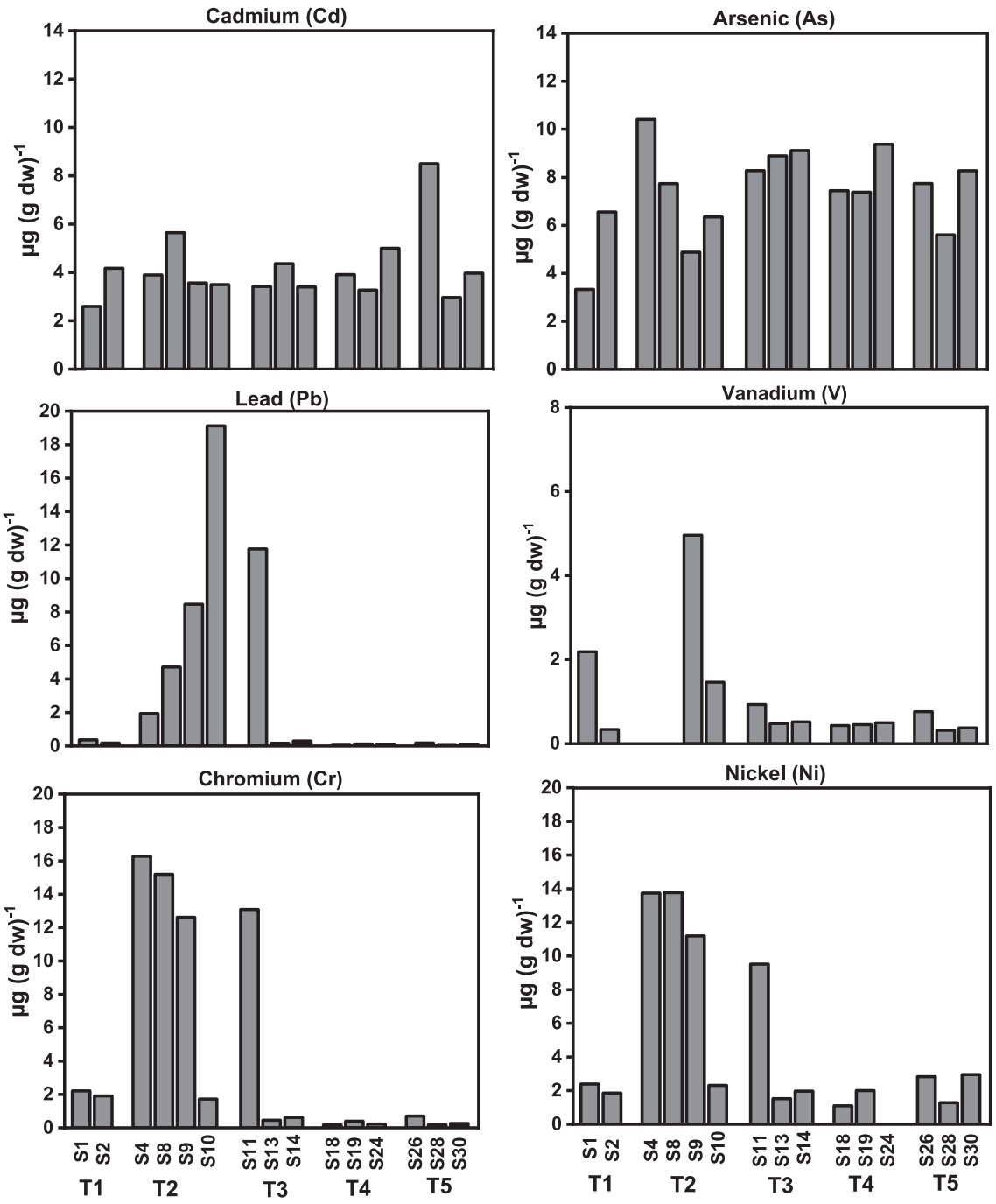

Fig. 6. Concentration of arsenic (As), cadmium (Cd), vanadium (V), chromium (Cr), nickel (Ni) and lead (Pb) measured in the >200 µm plankton size fraction at the transect stations (µg (g dw)$^{-1}$). Note different scales of the y-axis.

size fractions, whereas the concentration in station 6 was elevated in the 50–200 µm size fraction (Fig. 4). The concentrations in the smallest size fraction (0.7–20 µm) were below detection limit in all samples.

The average biomagnification factor (BMF) of Hg from the 20–50 µm to 50–200 µm plankton size fractions was ≤1 for most transects and stations, except for transects 2 where station 6 had a high concentration of Hg in the 50–200 µm size fraction (Fig. 4) resulting in a high range in the average BMF on this transect (Fig. 5). Similarly, for 20–50 to >200 µm size fraction BMF was close to 1 across all transects and in Disko Bay, except for a BMF of ca. 0.2 at NK where the Hg concentrations decreased strongly from the smallest to the largest size fraction (Fig. 4). Average BMF from the 50–200 µm to >200 µm size fractions was <1 for transects 2, 4, and NK, ca. 1 for transect 1, 3, 5 and AM and close to 2 for the Disko Bay station (Fig. 5).

3.3. Other metals/metalloids

There were no large differences between the stations in the concentrations of As, Cd or V in >200 µm size fraction (the only size fraction that was measured), although the concentration of V at station 9 was elevated (Fig. 6). The average concentrations of As, Cd and V were 7.7 ± 0.4, 4.1 ± 0.4, and 0.9 ± 0.3 µg (g dw) $^{-1}$, respectively. In contrast, concentrations of Cr (4.4 ± 1.6 µg (g dw)$^{-1}$), Ni (4.6 ± 1.2 µg (g dw) $^{-1}$), and Pb (3.2 ± 1.5 µg (g dw) $^{-1}$) were higher at stations on transect 2 and at station 11 on transect 3 than at other transects or stations. Particularly, the concentration of Pb increased from station 4 offshore towards

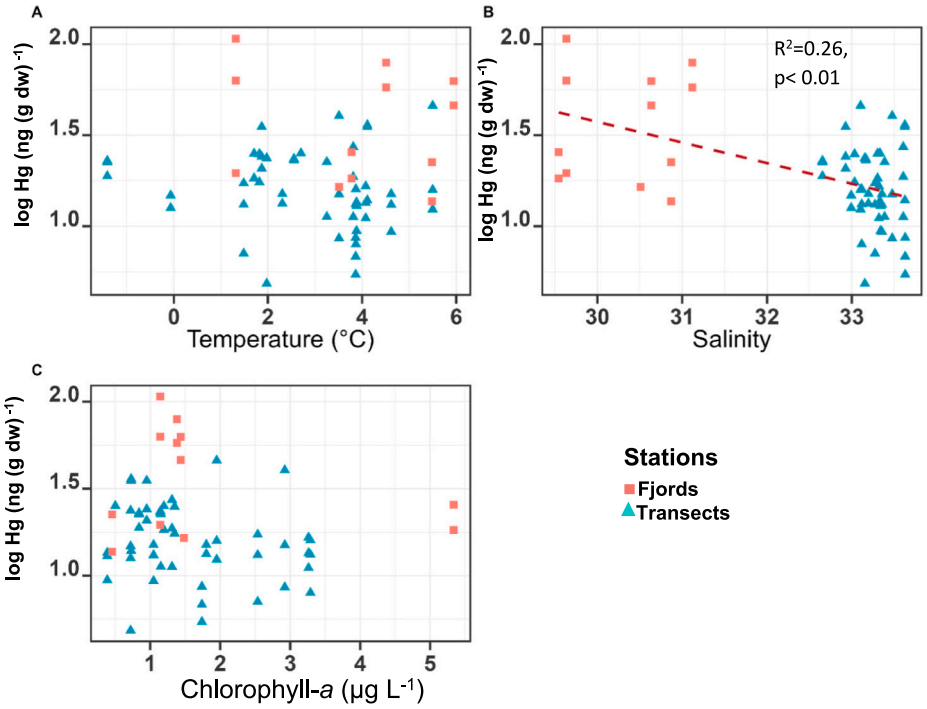

Fig. 7. Hg concentration in all plankton size fractions (ng (g dw)$^{-1}$) as a function of temperature (A; °C), salinity (B) and chlorophyll-*a* concentration (C; µg L^{-1}). (Red squares) fjord stations, (blue triangles) transect stations. The red line indicates the linear regression between the Hg and salinity ($p < 0.05$). (For interpretation of the references to colour in this figure legend, the reader is referred to the web version of this article.)

stations 10 and 11, which were located close to the coast (Fig. 6). The concentrations of other measured metals including Sc, Ti, Fe Co, Cu, Zn, Se, Pd, Ag, Sb, La, Pt, Au and Tl, generally increased towards the northern transects and were higher at stations closer to the coast than stations offshore (Suppl. Table 1).

3.4. Effect of salinity, temperature, chlorophyll-a concentration and zooplankton community structure on the mercury concentration

Hg concentrations were not related to temperature or chlorophyll-*a* in any of the plankton size fractions ($p > 0.05$), although the concentrations decreased slightly with increasing chlorophyll-*a* (Fig. 7). However, the Hg concentrations correlated negatively with the salinity ($p < 0.01$), although with a low R^2 of 0.26. This trend was mainly driven by the differences in salinity between the transect stations and fjords stations where the Hg concentrations were higher. Canonical Correspondence Analysis (CCA) showed no correlation between the Hg concentration in different size fractions (50–200 and >200 µm) and the abundance of specific zooplankton species ($F = 0.63$, $p > 0.05$, Fig. 8A). Similarly, the concentration of As, Pb, V, Ni or Cr were not related to the abundance of any specific species. However, Cd concentration correlated significantly with the total abundance of zooplankton ($F = 7.1$, $p < 0.05$, Fig. 8B), with a higher Cd concentration at the stations with lower zooplankton abundance. Also, Cd concentration in mesozooplankton correlated with the abundance of bivalves and harpacticoid copepods (Fig. 8B).

4. Discussion

4.1. Geographic differences in Hg concentration

Hg concentrations in phyto- and zooplankton in West Greenland were above the detection limit at all stations, although with a high (20-fold) variability between the stations and size fractions. The concentrations were comparable with the Hg concentrations measured in other parts of the Arctic Ocean, such as the Beaufort sea and the Amundsen Gulf, with recorded levels in pelagic particulate organic matter and zooplankton ranging from 12 to 206 ng (g dw)$^{-1}$ (Pućko et al., 2014). However, the Hg concentrations in our samples were considerably higher than the concentrations in phytoplankton (≥20 µm) and zooplankton (≥150 µm) from the Chukchi Sea (4–42.2 ng (g dw)$^{-1}$; Fox et al., 2017). The geographical variations in the Arctic phyto- and zooplankton Hg concentrations could be due to the difference in processes and activities modulating the transport and deposition of Hg (Dastoor et al., 2022; Kirk et al., 2012). For example, the atmospheric deposition, meltwater inflow, riverine and terrestrial run-offs, and anthropogenic activities may have differed at the sampling locations and seasons. In addition, oceanographic conditions, including temperature, organic carbon compositions, dissolved oxygen and nutrient concentrations influencing the distribution and speciation of Hg in marine ecosystems (Canário et al., 2017; Cossa et al., 2011) may have been different at the different sampling locations.

Specially, the small plankton size groups that have short generation times and fast uptake of Hg (Allen, 2016; Yao et al., 2020) would be expected to closely reflect the short-term changes in Hg concentrations. This might have been the case at the Disko Bay station, where we recorded the highest Hg concentration. This station was sampled during the early spring, possibly coinciding with the occurrence of the Atmospheric Mercury Depletion Event (the AMDE), known to trigger the scavenging and deposition of reactive Hg from the atmosphere onto the cryosphere. An increased Hg deposition on ice and water column during the freeze-melt periods could result in elevated uptake of Hg by the spring phytoplankton (including ice algae), with a resulting increase in the concentration of Hg in zooplankton that feeds on phytoplankton.

The higher Hg concentrations observed in fjord stations compared to transect stations could be due to the fjords acting as sinks for glacier meltwaters. Both fjords considered in this study receive substantial volumes of subglacial meltwaters from the Greenland Ice Sheet (Meire et al., 2015; Mortensen et al., 2020; Schuster et al., 2018). Thus, Hg concentrations in the fjords would be elevated, resulting in increased

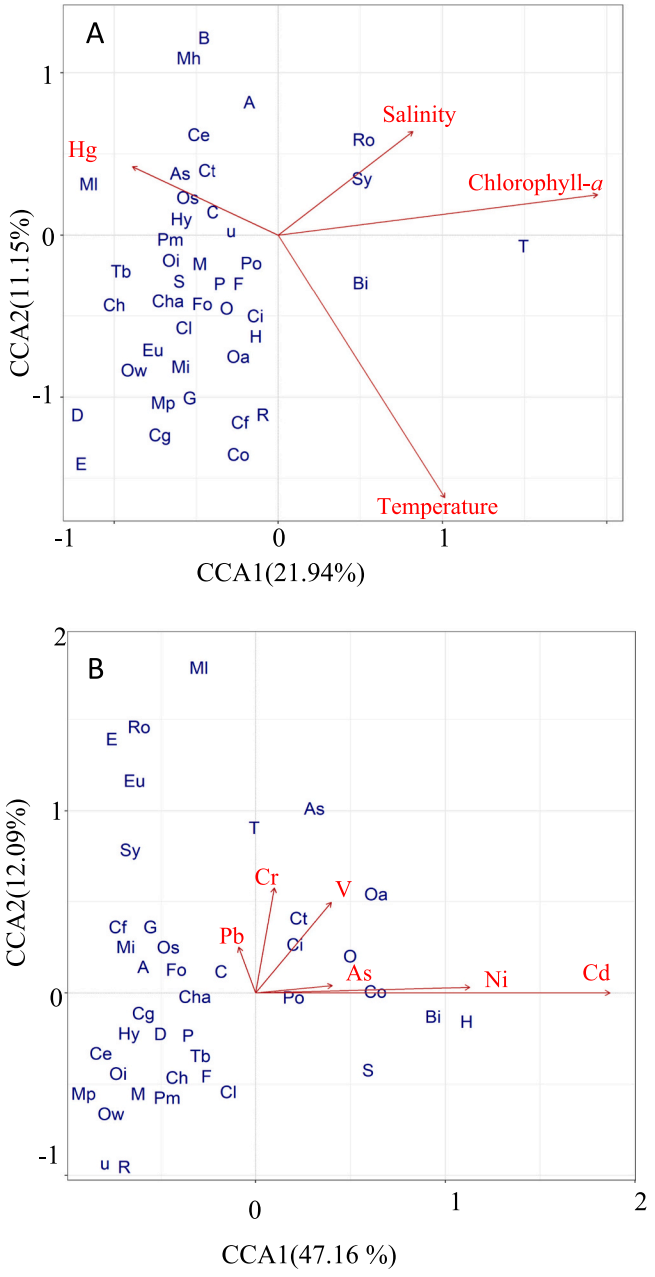

Fig. 8. Canonical Correspondence Analysis (CCA) ordination biplot of A) concentration of Hg in different size fractions and B) concentration of other metals in >200 μm size fraction (ng g^{-1} dw) together with the abundance of different zooplankton species (ind m^{-3}), salinity, chlorophyll-*a* (μg L^{-1}) and temperature (°C). Metal concentration and environmental variables are shown with red arrows, the letters indicate the abundance of different zooplankton species. The different axes represent percentages of the CCA1 (X-axis) and CCA2 (Y-axis). See Supplimentary Table 3 for species ID. (For interpretation of the references to colour in this figure legend, the reader is referred to the web version of this article.)

uptake by phytoplankton and their predators. This trend was also reflected within the fjords, with plankton samples closer to the fjord head having a generally higher Hg concentration than samples close to the mouth of the fjords, also reflected in the negative correlation between the salinity and Hg concentration. Fjords are also characterized by limited circulation compared with the open sea due to their topography, pronounced density gradients that lead to stratification, and a narrow opening at their mouth. With reduced circulation, the accumulation of heavy metals and other contaminants is more pronounced (Manzetti and Stenersen, 2010; Mortensen et al., 2011; Pitcher et al., 2021). Although there are limited comparable studies on the concentration of heavy metals in plankton from fjords and adjacent seas, our findings are consistent with studies by Azad et al. (2019) and Harman et al. (2019) on Norwegian marine ecosystems that reported higher Hg concentrations in fishes from pristine Norwegian fjords than in fishes from previously polluted open sea areas off the same coast. The findings were attributed to the characteristics of fjords, which made them more susceptible to heavy metal pollution than the open sea.

Besides the differences in the input of contaminants and the hydrographic characteristics of fjords, also other environmental factors or the zooplankton community composition could influence the geographic differences in metal concentrations. For instance, Chen et al. (2012) and Chen and Folt (2005) showed a pronounced correlation between chlorophyll-*a* or phytoplankton density and Hg concentration in plankton, with decreasing Hg concentrations with increasing chlorophyll-*a* concentration, indicating biodilution of Hg with increasing phytoplankton density. Also increasing temperatures have been shown to influence the Hg concentration through its effect on the metabolism of zooplankton, resulting in increased Hg accumulation at higher temperatures (Bai and Wang, 2020). However, we did not detect any obvious trends between temperature, chlorophyll-*a* and Hg concentration in plankton. Also, there was no correlation between the abundance of specific zooplankton species and Hg concentration, as also observed by Cardoso et al. (2013). However, evidence from freshwater suggests a role of community composition in Hg deposition so that both specific species, such as the cladoceran *Bosmina longirostris* and the cyclopoid *Thermocyclops brevifurcatus* (Long et al., 2018), and large size in general (Qin et al., 2023), could result in increased Hg concentration in plankton. Although our results did not indicate specific connections between the Hg concentration and zooplankton species, it seems plausible that traits such as size, lipid volume, or feeding mode could influence the Hg uptake and concentration of the zooplankton community (Gosnell et al., 2021; Twining and Fisher, 2004).

4.2. Trophic transfer of Hg

Our results showed no common patterns for the trophic transfer (BMF) between the different plankton size fractions, but in most cases, there either was no evidence of biomagnification (BMF of ca. 1) or the concentrations were decreasing in the higher size fractions (BMF < 1). This is in agreement with the results of Fox et al. (2017) and Pućko et al. (2014), who reported higher Hg concentrations in phytoplankton and particulate organic matter than in zooplankton. While we would expect Hg to be higher in the predator compared to the prey, a plausible explanation for the lack of biomagnification between the two larger size fractions could be that zooplankton species in these fractions occupied the same trophic level feeding on similar prey items, and thus had similar rates of Hg accumulation. The BMF < 1 could result from a depuration of Hg in mesozooplankton, either by excretion or in the faecal pellets. Several studies have documented the depuration of diverse metals, with up to 81 % of the ingested Hg from phytoplankton and particulate organic matter being depurated by zooplankton (Fisher et al., 1991; Lee and Fisher, 2017; Twining and Fisher, 2004; Yu et al., 2020). Nevertheless, this does not denigrate the trophic transfer of Hg. Previous studies have shown that while inorganic Hg (IHg) concentration decreases from phytoplankton to zooplankton, the concentration of methyl mercury (MeHg), which is the most toxic and bioavailable form of Hg species, increases from phytoplankton and particulate organic matter to zooplankton (Pućko et al., 2014; Watras and Bloom, 1992). This may be due to IHg binding more to the cellular membranes of phytoplankton, whereas MeHg binds to the cytoplasm due to its membrane permeability characteristics. The cellular membranes are usually assimilated but also excreted as part of the faecal pellet (Mason et al., 1995). Also, Pućko et al. (2014) identified the guts of zooplankton as hotspots for Hg methylation activities resulting in zooplankton

Table 1
Heavy metal concentration ranges in zooplankton from other marine areas (μg (g dw)$^{-1}$).

Location	As	Cd	Pb	V	Ni	Cr	Reference
West Greenland Coast	5.6–9.4	2.6–8.5	0.03–19.1	0.3–2.2	1.1–9.5	0.2–13.1	Present study
West Greenland	6						Bohn (1975)
Strathcona Sound	5.6–7.7	2.8–5.0					Bohn and McElroy (1976)
Kara sea (Arctic Ocean)	3.8–15.4	0.4–1.3	0.4–2.0	0.4–0.7	1.4–5.1	0.9–1.6	Lobus et al. (2018)
Laptev Sea (Arctic Ocean)	5.43–15.7	0.3–0.6		0.4–0.7	1.2–2.2	0.3–1.1	Lobus et al. (2019)
Tera Nova Bay (Anarctica)		1.6–7.1					Bargagli et al., 1996
Middle Eastern United states (Indian Ocean)						0.5–2.8	Greig (1975)
North Atlantic Ocean	14.5	9.8					Leatherland et al., 1973
Tyrrhenian Sea		0.3–0.6					Bargagli et al., 1996
Baltic Sea (Atlantic Ocean)		0.5–51	0.3–120		2.6–28.6	0.2–31.3	Brumann and Hennings (1994)
Kattegat (Atlantic Ocean)		0.6–8.9	2–122		1.3–9.7	0.6–32.4	
North Sea (Atlantic Ocean)		0.6–4.1	0.5–15.4		1.3–9.4	0.3–7.8	
NE Atlantic Ocean		2.8–14.6	1.0–28.1		1.3–18.3	0.3–12.3	
White Sea (Atlantic Ocean)	7.0–17	1.7–3.2	9.1–28.2	3.0–4.0	3.2–6.0	59–620	Leonova et al. (2013)
White Sea (Atlantic Ocean)	3.4–5.3	1.7–2.4	3.6–24	5.1–5.7	2.1–3	3.2–13	
Pacific		1.9–3.5	1.5–14.4		5–608	1–137	Martin and Knauer (1973)
Indian ocean	1.5–38	1.2–779			47–5500	160–400	Van Aswegen (2020)
Indian Ocean	1.5–22	1.2–79	3.8–35	1.2–79	47–750	160–430	

assimilating MeHg more efficiently than IHg and contributing efficiently to the transfer of MeHg to higher trophic levels organisms.

4.3. Trends in other heavy metals/metalloids

Similar to Hg, the concentrations of As, Cd, Pb, V, Ni, and Cr were always above the detection limit for the >200 μm size fraction. Of these, the concentrations of As were within the concentration range (3.8–15.4 μg (g dw)$^{-1}$) reported for zooplankton from other Arctic regions (Table 1), whereas the concentrations of Cd, Pb, V, Ni, and Cr were about 2–10 folds higher. Elevated concentrations of metals like Ni, Cr and V have previously been determined in marine sediment in West Greenland, most likely attributed to weathering of tertiary volcanic rocks in the area (Loring and Asmund, 1996). Other potential sources for metals in the west coast of Greenland could be shipping, atmospheric deposition or legacy mining. Particularly contributions from shipping are expected to increase in the near future since reducing sea ice will create alternative and more economically viable shipping routes (Gong and Barrie, 2005; Liu and Kronbak, 2010; Zhang et al., 2019). Since elevated heavy metal concentrations can cause oxidative and neural damage, reduce the reproductive abilities and feeding rates of zooplankton (Ensibi and Daly Yahia, 2017; Mohammed et al., 2010; Koski et al., 2017; Wang and Wang, 2010), potential discharges are problematic. In addition, as demonstrated by our measurements, arctic plankton can play an important role in modulating the transfer of bioavailable heavy metals to higher trophic level organisms such as fishes.

5. Conclusion

Our results demonstrate a high geographic variability in the concentration of Hg and other metals in plankton, suggesting an impact of riverine Hg transport (higher concentrations of Hg in fjords) and the role of AMDEs in Hg accumulation (higher concentrations of Hg in spring). It thus seemed that the geographic differences in the Hg concentrations in plankton could mainly be explained by the sources of Hg rather than environmental factors or zooplankton properties that could have modified the uptake and depuration of Hg. However, the Hg concentrations were in many cases higher in smaller planktonic size fractions than the larger plankton size fractions, suggesting depuration and thus the importance of community composition and metabolic activity of zooplankton. Our results emphasize the role of zooplankton in bioaccumulation and biomagnification of Hg in the Arctic food web and stress the need for continuous monitoring of Hg and other metals in Arctic marine plankton, especially in light of the changing climate.

Funding

This project has received funding from the European Union's Horizon 2020 research and innovation programme under grant agreement No 869383 (ECOTIP). The field trip to collect samples in the fjords was financed by the University of the Arctic - North 2 North Mobility Grant (UArctic). The field trip to Disko Bay was conducted in collaboration with the Greenland Ecosystem Monitoring (GEM; www.g-e-m.dk).

CRediT authorship contribution statement

Delove Abraham Asiedu: Data curation; Formal analysis; Investigation; Visualization; Writing - original draft. Jens Søndergaard: Formal analysis; Methodology (Sample analyses). Sigrun Jónasdóttir: Supervision; Validation; Conceptualization; Investigation; Writing - review & editing. Thomas Juul-Pedersen: Fund acquisition (North - North mobility grant); Writing - review & editing. Marja Koski: Supervision; Validation; Conceptualization; Investigation; Writing - review & editing; Funding acquisition, Project Coordinator (ECOTIP).

Declaration of competing interest

The authors declare that they have no known competing financial interests or personal relationships that could have appeared to influence the work reported in this paper.

Data availability

Data will be made available on request.

Acknowledgement

We wish to thank Else Ostermann and Mie Hylstofte Sichlau Winding for the assistance and logistic help during the fjord sampling, Sandra Drewes Fabricius for assistance in measuring the heavy metals and Torkel Gissel Nielsen for the Disko Bay samples. The Nuup Kangerlua sampling collection was conducted in collaboration with the marine monitoring program MarineBasis-Nuuk, part of Greenland Ecosystem Monitoring. Finally, we wish to thank the cruise leader Peter Munk as well as the captain and crew of R/V Dana, during the 6/21 ECOTIP West Greenland 2021 Cruise.

Appendix A. Supplementary data

Supplementary data to this article can be found online at https://doi.org/10.1016/j.marpolbul.2023.115436.

References

Achary, S., Panigrahi, S., Panigrahy, R.C., Prabhu, R.K., Sekar, J.K., Satpathy, K.K., 2020. Concentration factor of metals in zooplankton and their seasonality in Kalpakkam coast, southwest Bay of Bengal. Environ. Chem. Ecotoxicol. 2, 12–23. https://doi.org/10.1016/j.enceco.2020.01.002.

Alava, J.J., Gobas, F.A.P.C., 2012. Assessing biomagnification and trophic transport of persistent organic pollutants in the food chain of the Galapagos sea lion (Zalophus wollebaeki): conservation and management implications. In: New Approaches to the Study of Marine Mammals, pp. 77–108.

Allen, D.M., 2016. Zooplankton. In: Kennish, M.J. (Ed.), Encyclopedia of Estuaries. Encyclopedia of Earth Sciences Series. Springer. https://doi.org/10.1007/978-94-017-8801-4.

AMAP, 2011. Arctic Monitoring and Assessment Program 2011: Mercury in the Arctic. Arctic Monitoring and Assessment Programme (AMAP), Oslo, Norway xiv + 193 pp.

AMAP, 2018. AMAP Assessment 2018: Biological Effects of Contaminants on Arctic Wildlife and Fish. Arctic Monitoring and Assessment Programme (AMAP), Oslo, Norway vii+84pp.

Arctic Monitoring and Assessment Programme, 2009. AMAP assessment 2009: Human health in the Arctic. In: Arctic Monitoring and Assessment Programme (AMAP), Oslo, Norway xiv+254 pp. https://www.amap.no/documents/download/1163/inline.

Arendt, K.E., Juul-Pedersen, T., Mortensen, J., Blicher, M.E., Rysgaard, S., 2013. A 5-year study of seasonal patterns in mesozooplankton community structure in a sub-Arctic fjord reveals dominance of Microsetella norvegica (Crustacea, Copepoda). J. Plankton Res. 35 (1), 105–120. https://doi.org/10.1093/plankt/fbs087.

Arendt, K.E., Nielsen, T.G., Rysgaard, S., Tönnesson, K., 2010. Differences in plankton community structure along the Godthåbsfjord, from the Greenland ice sheet to offshore waters. Mar. Ecol. Prog. Ser. 401, 49–62. https://doi.org/10.3354/meps08368.

Ayala, D.J., Munk, P., Lundgreen, R.B.C., Traving, S.J., Jaspers, C., Jørgensen, T.S., Hansen, L.H., Riemann, L., 2018. Gelatinous plankton is important in the diet of European eel (Anguilla anguilla) larvae in the Sargasso Sea. Sci. Rep. 8 (1), 1–10. https://doi.org/10.1038/s41598-018-24388-x.

Azad, A.M., Frantzen, S., Bank, M. S, Johnsen, I.A., Tessier, E., Amouroux, D., Madsen, L., Maage, A., 2019. Spatial distribution of mercury in seawater, sediment, and seafood from the Hardangerfjord ecosystem, Norway. Sci. Total Environ. 667, 622–637. https://doi.org/10.1016/j.scitotenv.2019.02.352.

Bai, Z., Wang, M., 2020. Warmer temperature increases mercury toxicity in a marine copepod. Ecotoxicol. Environ. Saf. 201 https://doi.org/10.1016/j.ecoenv.2020.110861.

Bargagli, R., Nelli, L., Ancora, S., Focardi, S., 1996. Elevated cadmium accumulation in marine organisms from Terra Nova Bay (Antarctica). Polar Biol. 16, 513–520. https://doi.org/10.1007/BF02329071.

Bergmann, M., Collard, F., Fabres, J., Gabrielsen, G.W., Provencher, J.F., Rochman, C.M., van Sebille, E., Tekman, M.B., 2022. Plastic pollution in the Arctic. Nat. Rev. Earth Environ. 3 (5), 323–337. https://doi.org/10.1038/s43017-022-00279-8.

Bjerregaard, P., Johansen, P., Mulvad, G., Pedersen, H.S., Hansen, J.C., 2004. Lead sources in human diet in Greenland. Environ. Health Perspect. 112 (15), 1496–1498. https://doi.org/10.1289/ehp.7083.

Bohn, A., 1975. Arsenic in marine organisms from West Greenland. Mar. Pollut. Bull. 6 (6), 87–89. https://doi.org/10.1016/0025-326X(75)90150-2.

Bohn, A., McElroy, R.O., 1976. Trace metals (As, Cd, Cu, Fe, and Zn) in Arctic cod, Boreogadus saida, and selected zooplankton from Strathcona sound, northern Baffin Island. J. Fish. Res. Board Can. 33 (12), 2836–2840. https://doi.org/10.1139/f76-340.

Born, E.W., Bocher, J. (Eds.), 2001. The Ecology of Greenland. Greenl.: Ilinniusiorfik, Nuuk.

Bradley, R.S., Keimig, F.T., Diaz, H.F., 1992. Climatology of surface-based inversions in the north American Arctic. J. Geophys. Res. 97 (D14) https://doi.org/10.1029/92jd01451.

Brumann, L., Hennings, U., 1994. Metals in zooplankton from the Baltic Sea, 1980–84. Chem. Ecol. 9 (2), 87–103. https://doi.org/10.1080/02757549408038567.

Buch, E., 2002. Present Oceanographic Conditions in Greenland Waters. Danish Meteorological Institute. Scientific report.

Buch, E., Pedersen, S.A., Ribergaard, M.H., 2004. Ecosystem variability in West Greenland waters. J. Northwest Atl. Fish. Sci. 34 (September), 13–28. https://doi.org/10.2960/J.v34.m479.

Canário, J., Santos-Echeandia, J., Padeiro, A., Amaro, E., Strass, V., Klaas, C., Hoppema, M., Ossebaar, S., Koch, B.P., Laglera, L.M., 2017. Mercury and methylmercury in the Atlantic sector of the Southern Ocean. Deep Sea Res. Part II Top. Stud. Oceanogr. 138, 52–62. https://doi.org/10.1016/j.dsr2.2016.07.012.

Candelone, J.P., Hong, S., Pellone, C., Boutron, C.F., 1995. Post-industrial revolution changes in large-scale atmospheric pollution of the northern hemisphere by heavy metals as documented in central Greenland snow and ice. J. Geophys. Res. Atmos. 100 (D8), 16605–16616. https://doi.org/10.1029/95JD00989.

Cardoso, P.G., Marques, S.C., D'Ambrosio, M., Pereira, E., Duarte, A.C., Azeiteiro, U.M., Pardal, M.Â., 2013. Changes in zooplankton communities along a mercury contamination gradient in a coastal lagoon (Ria de Aveiro, Portugal). Mar. Pollut. Bull. 76 (1–2), 170–177. https://doi.org/10.1016/j.marpolbul.2013.09.007.

Castelao, R.M., Luo, H., Oliver, H., Rennermalm, A.K., Tedesco, M., Bracco, A., Yager, P. L., Mote, T.L., Medeiros, P.M., 2019. Controls on the transport of meltwater from the southern Greenland ice sheet in the Labrador Sea. J. Geophys. Res. Atmos. 124 (6), 3551–3560. https://doi.org/10.1029/2019JC015159.

Chen, C.Y., Folt, C.L., 2005. High plankton densities reduce mercury biomagnification. Environ. Sci. Technol. 39 (1), 115–121. https://doi.org/10.1021/es0403007.

Chen, C.Y., Driscoll, C.T., Lambert, K.F., Mason, R.P., Sunderland, E., 2012. Sources to seafood: mercury pollution in the marine environment. https://digitalcommons.library.umaine.edu/seagrant_pub/64?utm_source=digitalcommons.library.umaine.edu%2Fseagrant_pub%2F64&utm_medium=PDF&utm_campaign=PDFCoverPages.

Chételat, J., McKinney, M.A., Amyot, M., Dastoor, A., Douglas, T.A., Heimbürger-Boavida, L.E., Kirk, J., Kahilainen, K.K., Outridge, P.M., Pelletier, N., Skov, H., St. Pierre, K., Vuorenmaa, J., Wang, F., 2022. Climate change and mercury in the Arctic: abiotic interactions. Sci. Total Environ. 824 https://doi.org/10.1016/j.scitotenv.2022.153715.

Chevrollier, L.A., Koski, M., Søndergaard, J., Trapp, S., Aheto, D.W., Darpaah, G., Nielsen, T.G., 2022. Bioaccumulation of metals in the planktonic food web in the Gulf of Guinea. Mar. Pollut. Bull. 179 (January 2021) https://doi.org/10.1016/j.marpolbul.2022.113662.

Chouvelon, T., Strady, E., Harmelin-Vivien, M., Radakovitch, O., Brach-Papa, C., Crochet, S., Knoery, J., Rozuel, E., Thomas, B., Tronczynski, J., Chiffoleau, J.F., 2019. Patterns of trace metal bioaccumulation and trophic transfer in a phytoplankton-zooplankton-small pelagic fish marine food web. Mar. Pollut. Bull. 146, 1013–1030. https://doi.org/10.1016/j.marpolbul.2019.07.047.

Christie, P., Sommerkorn, M., 2012. RACER: Rapid Assessment of Circum-Arctic Ecosystem Resilience. WWF Global Arctic Programme, Ottawa, Canada.

Cossa, D., Heimbürger, L.E., Lannuzel, D., Rintoul, S.R., Butler, E.C.V., Bowie, A.R., Averty, B., Watson, R.J., Remenyi, T., 2011. Mercury in the Southern Ocean. Geochim. Cosmochim. Acta 75 (14), 4037–4052. https://doi.org/10.1016/j.gca.2011.05.001.

Dastoor, A., Wilson, S.J., Travnikov, O., Ryjkov, A., Angot, H., Christensen, J.H., Steenhuisen, F., Muntean, M., 2022. Arctic atmospheric mercury: sources and changes. Sci. Total Environ. 839 (March), 156213 https://doi.org/10.1016/j.scitotenv.2022.156213.

Dietz, R., Riget, F., Johansen, P., 1996. Lead, cadmium, mercury and selenium in Greenland marine animals. Sci. Total Environ. 186 (1–2), 67–93. https://doi.org/10.1016/0048-9697(96)05086-3.

Dietz, Rune, Outridge, P.M., Hobson, K.A., 2009. Anthropogenic contributions to mercury levels in present-day Arctic animals-A review. Sci. Total Environ. 407 (24), 6120–6131. https://doi.org/10.1016/j.scitotenv.2009.08.036.

Ensibi, C., Daly Yahia, M.N., 2017. Toxicity assessment of cadmium chloride on planktonic copepods Centropages ponticus using biochemical markers. Toxicol. Rep. 4, 83–88. https://doi.org/10.1016/j.toxrep.2017.01.005.

Fisher, N.S., Nolan, C.V., Fowler, S.W., 1991. Assimilation of metals in marine copepods and its biogeochemical implications. Mar. Ecol. Prog. Ser. 37–43.

Fox, A.L., Trefry, J.H., Trocine, R.P., Dunton, K.H., Lasorsa, B.K., Konar, B., Ashjian, C.J., Cooper, L.W., 2017. Mercury biomagnification in food webs of the northeastern Chukchi Sea, Alaskan Arctic. Deep Sea Res. Part II Top. Stud. Oceanogr. 144 (April), 63–77. https://doi.org/10.1016/j.dsr2.2017.04.020.

Gabrielli, P., Vallelonga, P., 2015. Contaminant records in ice cores. In: Environmental Contaminants: Using Natural Archives to Track Sources and Long-Term Trends of Pollution, pp. 393–430. https://doi.org/10.1007/978-94-017-9541-8_14.

Gong, S.L., Barrie, L.A., 2005. Trends of heavy metal components in the Arctic aerosols and their relationship to the emissions in the Northern Hemisphere. Sci. Total Environ. 342 (1–3), 175–183. https://doi.org/10.1016/j.scitotenv.2004.12.031.

González-Dávila, M., 1995. The role of phytoplankton cells on the control of heavy metal concentration in seawater. Mar. Chem. 48 (3–4), 215–236. https://doi.org/10.1016/0304-4203(94)00045-F.

Gosnell, K.J., Dam, H.G., Mason, R.P., 2021. Mercury and methylmercury uptake and trophic transfer from marine diatoms to copepods and field collected zooplankton. Mar. Environ. Res. 170 (May), 105446 https://doi.org/10.1016/j.marenvres.2021.105446.

Greig, R.A., 1975. Comparison of atomic absorption and neutron activation analyses for the determination of silver, chromium, and zinc in various marine organisms. Anal. Chem. 47 (9), 1682–1684. https://doi.org/10.1021/ac60359a003.

Harding, G., Dalziel, J., Vass, P., 2018. Bioaccumulation of methylmercury within the marine food web of the outer Bay of Fundy, Gulf of Maine. PLoS ONE 13 (7), 1–30. https://doi.org/10.1371/journal.pone.0197220.

Harman, C., Bekkby, T., Calabrese, S., Trannum, H., Oug, E., Hagen, A.G., Green, N., Kaste, Ø., Frigstad, H., 2019. The environmental status of norwegian coastal waters. In: World Seas: An Environmental Evaluation Volume I: Europe, the Americas and West Africa, Second Edi. Elsevier Ltd., pp. 69–84. https://doi.org/10.1016/B978-0-12-805068-2.00003-6

Hawkings, J.R., Linhoff, B.S., Wadham, J.L., Stibal, M., Lamborg, C.H., Carling, G.T., Lamarche-Gagnon, G., Kohler, T.J., Ward, R., Hendry, K.R., Falteisek, L., Kellerman, A.M., Cameron, K.A., Hatton, J.E., Tingey, S., Holt, A.D., Vinšová, P., Hofer, S., Bulínová, M., Spencer, R.G.M., 2021. Large subglacial source of mercury from the southwestern margin of the Greenland ice sheet. Nat. Geosci. 14 (7), 496–502. https://doi.org/10.1038/s41561-021-00753-w.

Hermanson, M.H., Brozowski, J.R., 2005. History of inuit community exposure to lead, cadmium, and mercury in sewage lake sediments. Environ. Health Perspect. 113 (10), 1308–1312. https://doi.org/10.1289/ehp.7985.

Iversen, T., Joranger, E., 1985. Arctic air pollution and large scale atmospheric flows. Atmos. Environ. 19 (12), 2099–2108. https://doi.org/10.1016/0004-6981(85)90117-9 (1967).

Johansen, P., Mulvad, G., Pedersen, H.S., Hansen, J.C., Riget, F., 2006. Accumulation of cadmium in livers and kidneys in Greenlanders. Sci. Total Environ. 372 (1), 58–63. https://doi.org/10.1016/j.scitotenv.2006.08.005.

Jørgensen, C.J., Søndergaard, J., Larsen, M.M., Kjeldsen, K.K., Rosa, D., Sapper, S.E., Albers, C.N., 2022. No Evidence for Large Subglacial Source of Mercury From the Southwestern Margin of the Greenland Ice Sheet. 10.31223/X5N04T.

Juul-Pedersen, T., Arendt, K.E., Mortensen, J., Blicher, M.E., Søgaard, D.H., Rysgaard, S., 2015. Seasonal and interannual phytoplankton production in a sub-Arctic tidewater outlet glacier fjord, SW Greenland. Mar. Ecol. Prog. Ser. 524, 27–38. https://doi.org/10.3354/meps11174.

Kehrig, H., do A., 2011. Mercury and plankton in tropical marine ecosystems: a review. Oecol. Aust. 15 (04), 869–880. https://doi.org/10.4257/oeco.2011.1504.07.

Kirk, J.L., Lehnherr, I., Andersson, M., Braune, B.M., Chan, L., Dastoor, A.P., Durnford, D., Gleason, A.L., Loseto, L.L., Steffen, A., St. Louis, V.L., 2012. Mercury in Arctic marine ecosystems: sources, pathways and exposure. Environ. Res. 119, 64–87. https://doi.org/10.1016/j.envres.2012.08.012.

Koski, M., Stedmon, C., Trapp, S., 2017. Ecological effects of scrubber water discharge on coastal plankton : potential synergistic effects of contaminants reduce survival and feeding of the copepod Acartia tonsa. Mar. Environ. Res. 129, 374–385. https://doi.org/10.1016/j.marenvres.2017.06.006.

Krabbenhoft, D.P., Sunderland, E.M., 2013. Global change and mercury. Science 341 (6153), 1457–1458. https://doi.org/10.1126/science.1242838.

Krawczyk, D.W., Witkowski, A., Juul-Pedersen, T., Arendt, K.E., Mortensen, J., Rysgaard, S., 2015. Microplankton succession in a SW Greenland tidewater glacial fjord influenced by coastal inflows and run-off from the Greenland Ice Sheet. Polar Biol. 38 (9), 1515–1533. https://doi.org/10.1007/s00300-015-1715-y.

Krawczyk, D.W., Meire, L., Lopes, C., Juul-Pedersen, T., Mortensen, J., Li, C.L., Krogh, T., 2018. Seasonal succession, distribution, and diversity of planktonic protists in relation to hydrography of the Godthåbsfjord system (SW Greenland). Polar Biol. 41 (10), 2033–2052. https://doi.org/10.1007/s00300-018-2343-0.

Lai, J., Zou, Y., Zhang, J., Peres-Neto, P.R., 2022. Generalizing hierarchical and variation partitioning in multiple regression and canonical analyses using the rdacca.hp R package. Methods Ecol. Evol. 13 (4), 782–788. https://doi.org/10.1111/2041-210X.13800.

Leatherland, T.M., Burton, J.D., Culkin, F., McCartney, M.J., Morris, R.J., 1973. Concentrations of some trace metals in pelagic organisms and of mercury in Northeast Atlantic Ocean water. In: Deep Sea Research and Oceanographic Abstracts, Vol. 20, No. 8. Elsevier, pp. 679–685. https://doi.org/10.1016/0011-7471(73)90085-5.

Lee, C.S., Fisher, N.S., 2017. Bioaccumulation of methylmercury in a marine copepod. Environ. Toxicol. Chem. 36 (5), 1287–1293. https://doi.org/10.1002/etc.3660.

Lehnherr, I., 2014. Methylmercury biogeochemistry: a review with special reference to Arctic aquatic ecosystems. Environ. Rev. 22 (3), 229–243. https://doi.org/10.1139/er-2013-0059.

Leonova, G.A., Bobrov, V.A., Bogush, A.A., Bychinskii, V.A., 2013. Concentration of chemical elements by zooplankton of the White Sea. Oceanology 53 (1), 54–70. https://doi.org/10.1134/S0001437013010086.

Li, Z., Chi, J., Wu, Z., Zhang, Y., Liu, Y., Huang, L., Lu, Y., Uddin, M., Zhang, W., Wang, X., Lin, Y., Tong, Y., 2022. Characteristics of plankton Hg bioaccumulations based on a global data set and the implications for aquatic systems with aggravating nutrient imbalance. Front. Environ. Sci. Eng. 16 (3), 1–13. https://doi.org/10.1007/s11783-021-1471-x.

Liu, M., Kronbak, J., 2010. The potential economic viability of using the Northern Sea route (NSR) as an alternative route between Asia and Europe. J. Transp. Geogr. 18 (3), 434–444. https://doi.org/10.1016/j.jtrangeo.2009.08.004.

Lobus, N.V., Drits, A.V., Flint, M.V., 2018. Accumulation of chemical elements in the dominant species of copepods in the Ob estuary and the adjacent shelf of the Kara Sea. Oceanology 58 (3), 405–415. https://doi.org/10.1134/S0001437018030104.

Lobus, Nikolay V., Arashkevich, E.G., Flerova, E.A., 2019. Major, trace, and rare-earth elements in the zooplankton of the Laptev Sea in relation to community composition. Environ. Sci. Pollut. Res. 26 (22), 23044–23060. https://doi.org/10.1007/s11356-019-05538-8.

Long, S.X., Hamilton, P.B., Yang, Y., Wang, S., Huang, W. da, Chen, C., Tao, R., 2018. Differential bioaccumulation of mercury by zooplankton taxa in a mercury-contaminated reservoir Guizhou China. Environ. Pollut. 239, 147–160. https://doi.org/10.1016/j.envpol.2018.04.008.

Loring, D.H., Asmund, G., 1996. Geochemical factors controlling accumulation of major and trace elements in Greenland coastal and fjord sediments. Environ. Geol. 28 (1), 2–11. https://doi.org/10.1007/s002540050072.

Macdonald, R.W., Bewers, J.M., 1996. Contaminants in the arctic marine environment: priorities for protection. ICES J. Mar. Sci. 53 (3), 537–563. https://doi.org/10.1006/jmsc.1996.0077.

Manić, L., Wallace, D., Onganer, P.U., Taalab, Y.M., Farooqi, A.A., Antonijević, B., Buha Djordjevic, A., 2022. Epigenetic mechanisms in metal carcinogenesis. Toxicol. Rep. 9 (February), 778–787. https://doi.org/10.1016/j.toxrep.2022.03.037.

Manzetti, S., Stenersen, V.H.J., 2010. A critical view of the environmental condition of the Sognefjord. Mar. Pollut. Bull. 60 (12), 2167–2174. https://doi.org/10.1016/j.marpolbul.2010.09.019.

Marnane, I., 2018. Mercury: a persistent threat to the environment and people's health. In: European Environment Agency Newsletter, 3.

Martin, J.H., Knauer, G.A., 1973. The elemental composition of plankton. Geochim. Cosmochim. Acta 37 (7), 1639–1653. https://doi.org/10.1016/0016-7037(73)90154-3.

Mason, R.P., Reinfelder, J.R., Morel, F.M., 1995. Bioaccumulation of mercury and methylmercury. Water Air Soil Pollut. 29 (8), 571. https://doi.org/10.1007/BF01189744.

Matias, R.S., Guímaro, H.R., Bustamante, P., Seco, J., Chipev, N., Fragão, J., Tavares, S., Ceia, F.R., Pereira, M.E., Barbosa, A., Xavier, J.C., 2022. Mercury biomagnification in an Antarctic food web of the Antarctic peninsula. Environ. Pollut. 304 https://doi.org/10.1016/j.envpol.2022.119199.

McConnell, J.R., Edwards, R., 2008. Coal burning leaves toxic heavy metal legacy in the Arctic. Proc. Natl. Acad. Sci. U. S. A. 105 (34), 12140–12144. https://doi.org/10.1073/pnas.0803564105.

McConnell, J.R., Chellman, N.J., Wilson, A.I., Stohl, A., Arienzo, M.M., Eckhardt, S., Fritzsche, D., Kipfstuhl, S., Opel, T., Place, P.F., Steffensen, J.P., 2019. Pervasive Arctic lead pollution suggests substantial growth in medieval silver production modulated by plague, climate, and conflict. Proc. Natl. Acad. Sci. U. S. A. 116 (30), 14910–14915. https://doi.org/10.1073/pnas.1904515116.

Meire, L., 2016. Biogeochemical Cycling in a Subarctic Fjord Adjacent to the Greenland Ice Sheet (Doctoral dissertation,. Ghent University.

Meire, L., Søgaard, D.H., Mortensen, J., Meysman, F.J.R., Soetaert, K., Arendt, K.E., Juul-Pedersen, T., Blicher, M.E., Rysgaard, S., 2015. Glacial meltwater and primary production are drivers of strong CO2 uptake in fjord and coastal waters adjacent to the Greenland ice sheet. Biogeosciences 12 (8), 2347–2363. https://doi.org/10.5194/bg-12-2347-2015.

Meire, Lorenz, Mortensen, J., Meire, P., Juul-Pedersen, T., Sejr, M.K., Rysgaard, S., Nygaard, R., Huybrechts, P., Meysman, F.J.R., 2017. Marine-terminating glaciers sustain high productivity in Greenland fjords. Glob. Chang. Biol. 23 (12), 5344–5357. https://doi.org/10.1111/gcb.13801.

Miner, K.R., D'Andrilli, J., Mackelprang, R., Edwards, A., Malaska, M.J., Waldrop, M.P., Miller, C.E., 2021. Emergent biogeochemical risks from Arctic permafrost degradation. Nat. Clim. Chang. 11 (10), 809–819. https://doi.org/10.1038/s41558-021-01162-y.

Mohammed, E.H., Wang, G., Jiang, J., 2010. The effects of nickel on the reproductive ability of three different marine copepods. Ecotoxicology 19, 911–916. https://doi.org/10.1007/s10646-010-0471-6.

Møller, E.F., Nielsen, T.G., 2020. Borealization of Arctic zooplankton—smaller and less fat zooplankton species in Disko Bay, Western Greenland. Limnol. Oceanogr. 65 (6), 1175–1188. https://doi.org/10.1002/lno.11380.

Møller, H.S., Jensen, K.G., Kuijpers, A., Aagaard-Sørensen, S., Seidenkrantz, M.S., Prins, M., Endler, R., Mikkelsen, N., 2006. Late-Holocene environment and climatic changes in Ameralik Fjord, Southwest Greenland: evidence from the sedimentary record. Holocene 16 (5), 685–695. https://doi.org/10.1191/0959683606hl963rp.

Mortensen, J., Lennert, K., Bendtsen, J., Rysgaard, S., 2011. Heat sources for glacial melt in a sub-Arctic fjord (Godthåbsfjord) in contact with the Greenland Ice Sheet. J. Geophys. Res. Atmos. 116 (1), 1–13. https://doi.org/10.1029/2010JC006528.

Mortensen, J., Rysgaard, S., Bendtsen, J., Lennert, K., Kanzow, T., Lund, H., Meire, L., 2020. Subglacial discharge and its Down-Fjord transformation in West Greenland Fjords with an Ice Mélange. J. Geophys. Res. Atmos. 125 (9), 1–13. https://doi.org/10.1029/2020JC016301.

Munk, P., Hansen, B.W., Nielsen, T.G., Thomsen, H.A., 2003. Changes in plankton and fish larvae communities across hydrographic fronts off West Greenland. J. Plankton Res. 25 (7), 815–830. https://doi.org/10.1093/plankt/25.7.815.

Munk, P., Hanse, K.E., Davies, J.M., Törnroos-Remes, A., Armitage, P., Jacquot, M., Bastian, D., Schmidt, C.E., Koziorowska-Makuch, K., Reinthaler, T., Amano, C., Baltar, F., Steenholdt, S., Svensen, C., Dietrich, U., Asiedu, D., Jónasdóttir, S., Koski, M., 2022. Report of the DANA 6/21 ECOTIP West Greenland 2021 Cruise: Investigations From Off Nuuk to North of Disko Island. Zenodo. https://doi.org/10.5281/zenodo.5913277.

Pawlowska, T.E., Charvat, I., 2004. Heavy-metal stress and developmental patterns of arbuscular mycorrhizal fungi. Appl. Environ. Microbiol. 70 (11), 6643–6649. https://doi.org/10.1128/AEM.70.11.6643-6649.2004.

Pitcher, G.C., Aguirre-velarde, A., Breitburg, D., Cardich, J., Carstensen, J., Conley, D.J., Dewitte, B., Engel, A., Flores, G., Espinoza-morriber, D., Graco, M., Gr, M., Guti, D., Huang, H.M., Isensee, K., Elena, M., Levin, L., Lorenzo, A., Machu, E., Zhu, Z.Y., 2021. Progress in Oceanography System Controls of Coastal and Open Ocean Oxygen Depletion, p. 197. https://doi.org/10.1016/j.pocean.2021.102613.

Pućko, M., Burt, A., Walkusz, W., Wang, F., Macdonald, R.W., Rysgaard, S., Barber, D.G., Tremblay, J.É., Stern, G.A., 2014. Transformation of mercury at the bottom of the arctic food web: an overlooked puzzle in the mercury exposure narrative. Environ. Sci. Technol. 48 (13), 7280–7288. https://doi.org/10.1021/es404851b.

Pućko, M., Stern, G.A., Macdonald, R.W., Jantunen, L.M., Bidleman, T.F., Wong, F., Barber, D.G., Rysgaard, S., 2015. The delivery of organic contaminants to the Arctic food web: why sea ice matters. Sci. Total Environ. 506–507, 444–452. https://doi.org/10.1016/j.scitotenv.2014.11.040.

Qin, F., Amyot, M., Bertolo, A., 2023. The relationship between zooplankton vertical distribution and the concentration of aqueous hg in boreal lakes: a comparative field study. Sci. Total Environ. 858, 159793 https://doi.org/10.1016/j.scitotenv.2022.159793.

Rigét, F., Mosbech, A., Boertmann, D., Wegeberg, S., Merkel, F., Aastrup, P., Christensen, T., Ugarte, F., Hedeholm, R., Fritt-Rasmussen, J., 2018. The seas around Greenland: an environmental status and future perspective. In: World Seas: An Environmental Evaluation Volume I: Europe, the Americas and West Africa, Second Edi. Elsevier Ltd. https://doi.org/10.1016/B978-0-12-805068-2.00001-2

Rykova, T., Straneo, F., Bower, A.S., 2015. Seasonal and interannual variability of the West Greenland current system in the Labrador Sea in 1993–2008. J. Geophys. Res. Atmos. 120, 1318–1332. https://doi.org/10.1002/2014JC010386.

Schuster, P.F., Schaefer, K.M., Aiken, G.R., Antweiler, R.C., Dewild, J.F., Gryziec, J.D., Gusmeroli, A., Hugelius, G., Jafarov, E., Krabbenhoft, D.P., Liu, L., Herman-Mercer, N., Mu, C., Roth, D.A., Schaefer, T., Striegl, R.G., Wickland, K.P., Zhang, T., 2018. Permafrost stores a globally significant amount of mercury. Geophys. Res. Lett. 45 (3), 1463–1471. https://doi.org/10.1002/2017GL075571.

Schwaba, T., Bleidorn, W., Hopwood, C.J., Gebauer, J.E., Rentfrow, P.J., Potter, J., Gosling, S.D., 2021. The impact of childhood lead exposure on adult personality: evidence from the United States, Europe, and a large-scale natural experiment. Proc. Natl. Acad. Sci. U. S. A. 118 (29), 1–7. https://doi.org/10.1073/pnas.2020104118.

Sterman, N.T., 1988. Spectrophotometric and fluorometric chlorophyll analysis. In: Lobban, C.S., Chapman, D.J., Kremer, B.P. (Eds.), Experimental phycology: a laboratory manual. Cambridge Univ. Press, New York, pp. 35–46.

Steffen, Alexandra, Schroeder, W., Macdonald, R., Poissant, L., Konoplev, A., 2005. Mercury in the Arctic atmosphere: an analysis of eight years of measurements of GEM at alert (Canada) and a comparison with observations at Amderma (Russia) and Kuujjuarapik (Canada). Sci. Total Environ. 342 (1–3), 185–198. https://doi.org/10.1016/j.scitotenv.2004.12.048.

Steffen, A., Douglas, T., Amyot, M., Ariya, P., Aspmo, K., Berg, T., Bottenheim, J., Brooks, S., Cobbett, F., Dastoor, A., Dommergue, A., Ebinghaus, R., Ferrari, C., Gardfeldt, K., Goodsite, M.E., Lean, D., Poulain, A.J., Scherz, C., Skov, H., Temme, C., 2008. A synthesis of atmospheric mercury depletion event chemistry in the atmosphere and snow. Atmos. Chem. Phys. 8 (6), 1445–1482. https://doi.org/10.5194/acp-8-1445-2008.

Stohl, A., 2006. Characteristics of atmospheric transport into the Arctic troposphere. J. Geophys. Res. Atmos. 111 (11), 1–17. https://doi.org/10.1029/2005JD006888.

Stuart-Lee, A.E., Mortensen, J., Kaaden, A.S.va. der, Meire, L., 2021. Seasonal hydrography of Ameralik: a Southwest Greenland Fjord impacted by a land-terminating glacier. J. Geophys. Res. Atmos. 126 (12), 1–17. https://doi.org/10.1029/2021JC017552.

Troell, M., Eide, A., Isaksen, J., Hermansen, Ø., Crépin, A.S., 2017. Seafood from a changing Arctic. Ambio 46 (Caff 2013), 368–386. https://doi.org/10.1007/s13280-017-0954-2.

Twining, B.S., Fisher, N.S., 2004. Trophic transfer of trace metals from protozoa to mesozooplankton. Limnol. Oceanogr. 49 (1), 28–39. https://doi.org/10.4319/lo.2004.49.1.0028.

UN-Environment, 2019. Global Mercury Assessment 2018. UN-Environment Programme, Chemicals and Health Branch, Geneva, Switzerland, p. 59.

Van Aswegen, J.D., 2020. Metal Composition of Zooplankton From the Western Indian Ocean. Doctoral dissertation,. North-West University, South Africa.

Walsh, J.E., Anisimov, O., Hagen, J.M.O., Jakobsson, T., Oerlemans, J., Prowse, T.D., Romanovsky, V., Savelieva, N., Serreze, M., Alex, S., Igor, S., Solomon, S., 2005. Cryosphere and hydrography. Chapter 6. In: Arctic Climate Impact Assessment (ACIA). Cambridge University Press, London, pp. 183–242.

Wang, M., Wang, G., 2010. Oxidative Damage Effects in the Copepod Tigriopus Japonicus Mori Experimentally Exposed to Nickel, pp. 273–284. https://doi.org/10.1007/s10646-009-0410-6.

Watras, C.J., Bloom, N.S., 1992. Mercury and methylmercury in individual implications for bioaccumulation zooplankton. Limnol. Oceanogr. 37 (6), 1313–1318. https://doi.org/10.4319/lo.1992.37.6.1313.

World Health Organisation, 2017. Risks from mercury for human health and the environment Risks from mercury for human health and the environment Report of an awareness-raising. Mercury 3 (September).

Xu, Y., Wang, W.X., 2003. Fates of diatom carbon and trace elements by the grazing of a marine copepod. Mar. Ecol. Prog. Ser. 254, 225–238. https://doi.org/10.3354/meps254225.

Yao, C., He, T., Xu, Y., Ran, S., Qian, X., Long, S., 2020. Mercury bioaccumulation in zooplankton and its relationship with eutrophication in the waters in the karst region of Guizhou Province, Southwest China. Environ. Sci. Pollut. Res. 27 (8), 8596–8610. https://doi.org/10.1007/s11356-019-07479-8.

Yu, Z.G., Zhang, L., Wu, Y., Jin, B., 2020. Efflux behavior of inorganic mercury and methylmercury in the marine copepod Tigriopus japonicus. Sci. Total Environ. 703, 135655 https://doi.org/10.1016/j.scitotenv.2019.135655.

Zhang, Y., Lu, X., Wang, N., Xin, M., Geng, S., Jia, J., Meng, Q., 2016. Heavy metals in aquatic organisms of different trophic levels and their potential human health risk in Bohai Bay, China. Environ. Sci. Pollut. Res. 23 (17), 17801–17810. https://doi.org/10.1007/s11356-016-6948-y.

Zhang, J., Zhou, F., Chen, C., Sun, X., Shi, Y., Zhao, H., Chen, F., 2018. Spatial distribution and correlation characteristics of heavy metals in the seawater, suspended particulate matter and sediments in Zhanjiang Bay, China. PLoS ONE 13 (8), 1–25. https://doi.org/10.1371/journal.pone.0201414.

Zhang, Q., Wan, Z., Hemmings, B., Abbasov, F., 2019. Reducing black carbon emissions from Arctic shipping : solutions and policy implications. J. Clean. Prod. 241, 118261 https://doi.org/10.1016/j.jclepro.2019.118261.

Zulaikhah, S.T., Wahyuwibowo, J., Pratama, A.A., 2020. Mercury and its effect on human health: a review of the literature. Int. J. Public Health Res. 9 (2), 103–114. https://doi.org/10.11591/ijphs.v9i2.20416.